Remote Sensing of Environment 113 (2009) 1899–1911

Contents lists available at ScienceDirect

Remote Sensing of Environment

journal homepage: www.elsevier.com/locate/rse

Estimating the altitude of aerosol plumes over the ocean from reflectance ratio measurements in the O_2 A-band

Philippe Dubuisson [a,*], Robert Frouin [b], David Dessailly [c], Lucile Duforêt [c], Jean-François Léon [a], Kenneth Voss [d], David Antoine [e]

[a] Laboratoire d'Optique Atmopshérique, Univsersité de Lille I, 59655 Villeneuve d'Ascq Cedex, France
[b] Scripps Institution of Oceanography, University of California San Diego, La Jolla, California 92093-0224, USA
[c] Ecosystèmes Littoraux et Cotiers, Université du Littoral Cote d'Opale, 32 Avenue Foch, 62930 Wimereux, France
[d] Department of Physics, University of Miami, Coral Gables, Florida 33124, USA
[e] Laboratoire d'Océanographie de Villefranche, Observatoire Océanologique de Villefranche, Quai de la Darse, 06238 Villefranche-sur-Mer, France

ARTICLE INFO

Article history:
Received 12 August 2008
Received in revised form 18 March 2009
Accepted 25 April 2009

Keywords:
Aerosols
Vertical distribution
Oxygen A-band
Scattering
Absorption
MERIS
POLDER

ABSTRACT

A methodology is proposed to infer the altitude of aerosol plumes over the ocean from reflectance ratio measurements in the O_2 absorption A-band (759 to 770 nm). The reflectance ratio is defined as the ratio of the reflectance in a first spectral band, strongly attenuated by O_2 absorption, and the reflectance in a second spectral band, minimally attenuated. For a given surface reflectance, simple relations are established between the reflectance ratio and the altitude of an aerosol layer, as a function of atmospheric conditions and the geometry of observation. The expected accuracy for various aerosol loadings and models is first quantified using an accurate, high spectral resolution, radiative transfer model that fully accounts for interactions between scattering and absorption. The method is developed for POLDER and MERIS, satellite sensors with adequate spectral characteristics. The simulations show that the method is only accurate over dark surfaces when aerosol optical thickness at 765 nm is relatively large (>0.3). In this case, the expected accuracy is on the order of ± 0.5 km or ± 0.2 km for POLDER or MERIS respectively. More accurate estimates are obtained with MERIS, since in this case the spectral reflectance ratio is more sensitive to aerosol altitude. However, a precise spectral calibration is needed for MERIS. The methodology is applied to MERIS and POLDER imagery acquired over marine surfaces. The estimated aerosol altitude is compared with *in situ* lidar profiles of backscattering coefficient measured during the AOPEX-2004 experiment for MERIS, or obtained with the space-borne lidar CALIOP for POLDER. The retrieved altitudes agree with lidar measurements in a manner consistent with theory. These comparisons demonstrate the potential of the differential absorption methodology for obtaining information on aerosol altitude over dark surfaces.

1. Introduction

Aerosol vertical distribution is a key parameter for radiative forcing studies, for remote sensing applications, or for air quality forecasts (Al-Saadi et al., 2005; Boucher, 2002; Liao & Seinfeld, 1998). Scattering by mineral particles affects the direct aerosol forcing in the longwave spectral region during dust events, but the effect strongly depends on the altitude of the particles (Dufresne et al., 2002). Aerosol scavenging, therefore the indirect radiative forcing, is determined by the relative location of aerosols and clouds in the vertical (Boucher, 2002). Knowledge of aerosol vertical structure is also important for inversion of satellite data since it affects the reflectance measured at the top of the atmosphere. In this respect, several studies have shown the impact of aerosol vertical structure on the performance of standard atmospheric correction algorithms in ocean color remote sensing, especially in the presence of absorbing particles (Duforêt et al., 2007; Gordon, 1997; Gordon et al., 1997).

A detailed knowledge of the vertical structure of scatterers is available from Lidar techniques. Ground-based Lidar networks, such as the European Aerosol Research Lidar NETwork (EARLINET) or the Micro-Pulse Lidar NETwork (MPLNET) can be used to obtain vertical profiles at the local scale (Schneider et al., 2000). At global scale, lidars of the Cloud-Aerosol Lidar and Infrared Pathfinder Satellite Observation (CALIPSO) (Winker et al., 2003) and Ice, Cloud, and land Elevation Satellite (ICESat) missions (Zwally et al., 2002) allow one to estimate the vertical distribution of scatterers, but over a limited spatial swath. In addition, methodologies have been proposed to provide information on the aerosol vertical distribution from passive remote sensing measurements. As an example, techniques based on a limb-scanning mode have been applied to the Stratospheric Aerosols and Gas Experiment (SAGE) radiometer, but can hardly be extended to the lower troposphere (Brogniez et al., 2002).

* Corresponding author. Fax: +33 3 20 43 43 42.
E-mail address: Philippe.Dubuisson@univ-lille1.fr (P. Dubuisson).

0034-4257/$ – see front matter © 2009 Elsevier Inc. All rights reserved.
doi:10.1016/j.rse.2009.04.018

In the spectral range of the oxygen A-band (759 to 770 nm), the reflected solar radiation measured at the top of the atmosphere depends mainly on oxygen absorption, surface reflectance, and vertical distribution of scatterers. Methods exploiting spectral variations of absorption in the oxygen A-band, using a moderate spectral resolution, have been proposed by Badayev and Malkevich (1978) to retrieve the aerosol vertical profile and applied by Gabella et al. (1997, 1999) to the Modular Optoelectronic Scanner (MOS) instrument (Zimmermann et al., 1993). In this approach, several bands (four bands in the oxygen A-band for MOS), with a moderate spectral resolution (1 nm), are used. In the case of instruments using only two large spectral bands in the oxygen A-band, such as the Polarization and Directionality of the Earth's Reflectance POLDER (Deschamps et al., 1994) instrument (10 nm and 40 nm width), methodologies based on reflectance ratio have been proposed for surface pressure or cloud altitude retrievals (Barton & Scott, 1986; Chance, 1997). This approach remains very simple, because it is based on two spectral bands and a common viewing angle, and is applicable to the large swath of the sensors thus allowing a wide spatial coverage. Previous studies have shown the potential of such an approach for the determination of surface pressure (Bréon & Bouffiès, 1996; Dubuisson et al., 2001; Van Diedenhoven et al., 2005) or cloud top altitude (Fischer & Grassl, 1991; Vanbauce et al., 1998) from satellite sensors with adequate spectral characteristics, such as POLDER, the MEDium Resolution Imaging Spectrometer (MERIS) (Rast et al., 1999), or The SCanning Imaging Absorption SpectroMeter for Atmospheric CHartographY (SCIAMACHY). As a complement to the previous studies, influence of aerosol altitude on the degree of linear polarization of the zenith skylight has been highlighted in the spectral region of the O_2 A-band (Boesche et al., 2008).

This paper reports on the potential of using reflectance ratio measurements in the O_2 A-band (i.e. a differential absorption technique) for estimating aerosol altitude from space. In Section 2 the method, as well as the radiative transfer model used in the simulations, are described. The expected accuracy is then estimated through a sensitivity study. In Section 3 the proposed methodology is applied to imagery from POLDER and MERIS, instruments that have adequate spectral properties in the spectral range of the O_2 A-band (see Section 2.1). Altitude retrievals are first presented using POLDER measurements, for aerosol plumes over the Atlantic Ocean. POLDER measurements offer the opportunity to compare estimates of aerosol altitude with observations of the CALIOP lidar, in the context of the A-train. The methodology is also applied to MERIS imagery acquired in July–August 2004 over the western Mediterranean Sea during the AOPEX experiment (Antoine et al., 2006). Estimates of aerosol altitude from MERIS data are compared with *in situ* lidar profiles of backscattering coefficient, measured onboard ship during the campaign. Results and accuracy of retrievals are discussed. A perspective is given on the operational applicability of the method.

2. Potential of the O_2 A-band for aerosol altitude retrieval

2.1. Methods and principles

The method proposed to retrieve aerosol altitude exploits the coupling between aerosol scattering and oxygen absorption in the A-band centered on 760 nm (Dubuisson et al., 2001; Van Diedenhoven et al., 2005). The top-of-atmosphere (TOA) reflectance measured in that band depends on the altitude of the atmosphere scatterers, especially aerosols. The higher the aerosols, the larger the reflectance, since a number of photons are backscattered to space instead of absorbed by oxygen in the lower layers. In addition, the coupling between aerosol scattering and oxygen absorption, which enhances absorption, is less effective in this case because there are fewer molecules. Instead of using reflectance, one can use the ratio R of the reflectance influenced by oxygen absorption and the reflectance measured outside of the absorption band or in a spectral region minimally influenced by oxygen absorption. This is convenient to reduce the impact of aerosol scattering and uncertainties due radiometric calibration, though only accurate inter-band calibration is needed. Of course, only one piece of information about aerosol vertical structure can be obtained using R, i.e., an average aerosol altitude, Z_a. In this study, an accuracy $\Delta Z_a < 0.5$ km on the aerosol layer altitude is expected, as an example based on requirements needed for ocean color applications (Duforêt et al., 2007).

Fig. 1 presents the oxygen transmission in the O_2 A-band. The computations were made using a line-by-line code, in which the spectroscopic parameters for oxygen lines are specified from HITRAN 2004 database (Rothman et al., 2005). The POLDER and MERIS instrument have adequate spectral response in the oxygen A-band near 760 nm for measurements of the reflectance ratio R. For the POLDER instrument, the spectral bands are centered at 763 nm (10 nm

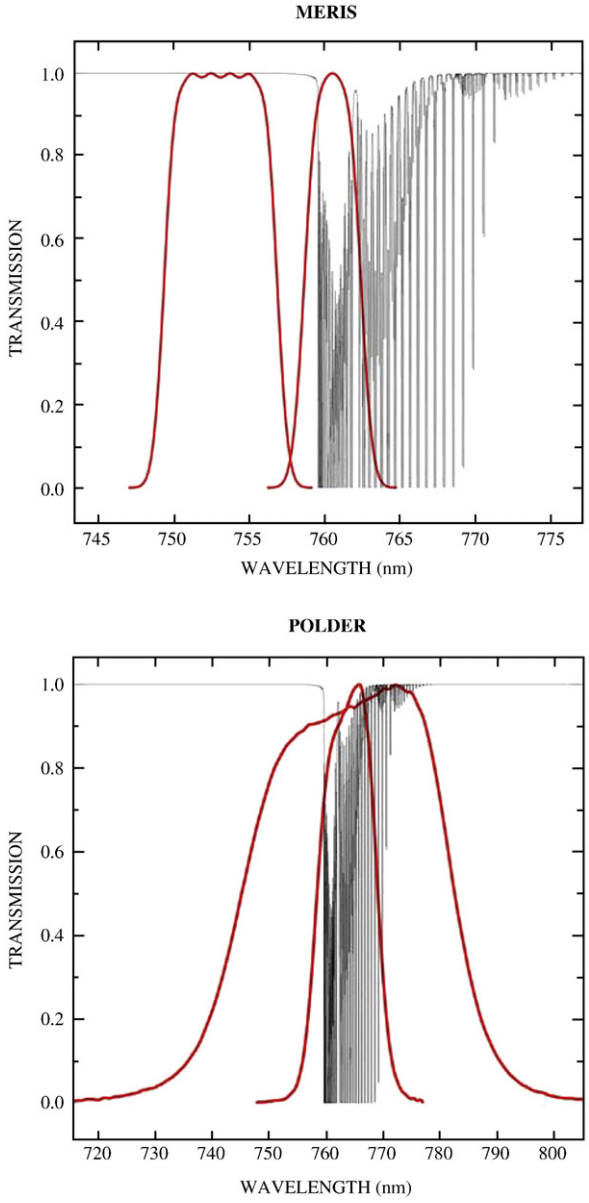

Fig. 1. Spectral transmission (red lines) of the MERIS or POLDER spectral bands located in the region of the oxygen A-band. The line-by-line transmission of oxygen (black lines) is reported for an airmass of 2. (For interpretation of the references to colour in this figure legend, the reader is referred to the web version of this article.)

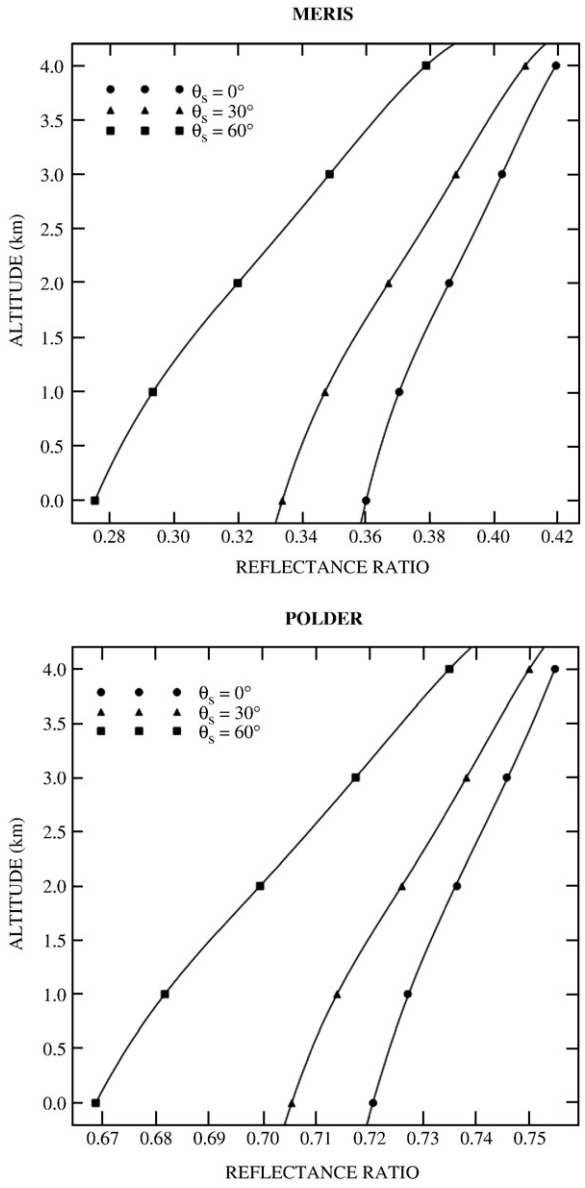

Fig. 2. Altitude of a 1 km dust aerosol layer as a function of the reflectance ratio R, for various solar zenith angles θ_s. Simulations have been performed for MERIS (upper curve) or POLDER (lower curve), over a marine surface, with a line-by-line code, using the following conditions: a view zenith angle of 30°, in the forward peak of scattering and with an aerosol optical thickness of 0.3 at 765 nm. The reflectance ratio R is defined as the ratio of the reflectance measured in the channel centered in the oxygen absorption band and the reflectance measured in the close non-absorbing (for MERIS) or less absorbing (for POLDER) channel (see Fig. 1).

wide) and 765 nm (40 nm wide). The POLDER narrow band is strongly attenuated by oxygen absorption, whereas the wide band is only partially attenuated. The spectral characteristics of MERIS are more adequate for application of the differential absorption method, with a non-absorbing channel centered at 753.75 nm (7.5 nm wide) next to an absorbing channel centered at 761.75 nm (3.75 nm wide). A spectral characterization of MERIS was performed before launch, but spectral shifts have been observed, with a maximal spectral dispersion of about 1 nm. However, the retrieval of apparent pressure in the O_2 A-band needs an accurate knowledge of the spectral characteristics of MERIS bands (Dubuisson et al., 2001). Methodologies have been developed and validated for a spectral calibration of MERIS in the oxygen A-band, with an accuracy of 0.01 nm (Casadio & Colagrande, 2004; Dubuisson et al., 2003; Ramon et al., 2003).

To investigate the relation between reflectance ratio R and aerosol altitude Z_a, the TOA reflectance was simulated using an accurate radiative transfer code referred to as GAME (Dubuisson et al., 1996). In this code, gaseous absorption, calculated using the line-by-line code, is fully coupled with molecule and aerosol scattering. Multiple scattering effects are treated with the Discrete Ordinates Method (Stamnes et al., 1988). In this approach, the radiative transfer equation is solved assuming a vertically inhomogeneous atmosphere stratified into plane-parallel and homogeneous layers. Over marine surfaces, an accurate treatment of sea surface roughness, caused by wind, is included using a wave-slope probability density (Cox & Munk, 1954). The interactions with the atmospheric radiance field are taken into account using the Adding Doubling Method (DeHaan et al., 1987; Duforêt et al., 2007).

The simulations indicate that the altitude of an aerosol layer Z_a can be related to the reflectance ratio R, as least in theory, if other parameters are known, mainly the surface reflectance, oxygen absorption, and optical properties of scatterers. In this case, Fig. 2 shows that Z_a can be expressed directly as a function of R through simple parameterizations. These parameterizations depend on surface reflectance, solar and viewing geometry, and the main aerosol optical properties: aerosol optical thickness δ_a, single scattering albedo ϖ_0 and asymmetry factor g. Fig. 2 indicates a higher sensitivity of the ratio R to the altitude of the aerosol layer for MERIS, due to its spectral definition, or for larger solar zenith angles (or view zenith angles by the reciprocity principle) caused by airmass effects. Indeed, Fig. 2 shows that the range of the reflectance ratio is about twice as large for MERIS than for POLDER using the same atmospheric conditions and geometry of observation. Based on the parameterizations $Z_a = f(R)$ presented in Fig. 2, a simple algorithm has been defined to retrieve Z_a from R and from look-up-tables (LUTs). They have been established assuming a wide range of surface parameters, solar and view geometries and aerosol characteristics (see Section 3.1 and Fig. 3 for algorithm details). The availability of the atmospheric or surface parameters will be discussed in Section 3. Note that the contribution of the atmosphere to the TOA reflectance is predominant over dark surfaces, due to scattering processes. The proposed method is then expected to be more efficient in this case. Especially favorable conditions can be found over ocean, for which the reflectance of the marine surface is generally close to zero at 760 nm. The main difficulty in this case resides in the strong variability and uncertainties in atmospheric parameters. On the contrary, photons coming from the surface are predominant in the case of bright surfaces. The method is therefore less accurate in that case. A sensitivity study is presented in the following section to quantify the expected accuracy of the method.

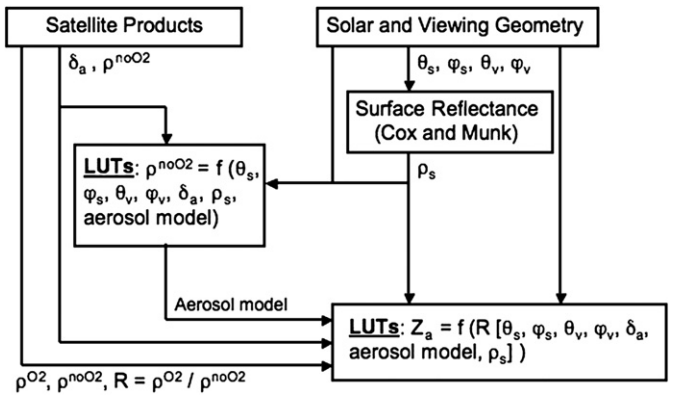

Fig. 3. Flowchart of the algorithm proposed for aerosol altitude retrievals from measurements and simulations of the reflectance ratio R in the O_2 A-band (see Section 3.1 for details). ρ^{O2} and ρ^{noO2} are the reflectances measured in the oxygen absorption channel and in the non-absorbing channel, respectively. A wind speed of 12 m s^{-1} has been used for LUTs calculations.

2.2. Sensitivity study

An analysis has been performed from the pre-computed LUTs, to evaluate the theoretical accuracy of the proposed method, as well as its sensitivity to the main parameters. First, assuming that all parameters are well known, the numerical accuracy due to interpolation is on the order of 0.01 km and can be considered as negligible. The theoretical accuracy ΔZ_a on the retrieved altitude has been then evaluated as a function of the aerosol optical thickness, assuming an accuracy of 0.5% on the radiometric calibration of the reflectance ratio R (Hagolle et al., 1999). In these conditions, the spectral accuracy is given in Table 1. It is about 0.1 km for larger aerosol optical thickness δ_a at 765 nm (i.e. $\delta_a > 0.3$) with MERIS. Uncertainties are bigger with the POLDER instrument, due to its spectral definition, i.e., on the order of 0.2 km. The MERIS instrument has a better sensitivity and the expected accuracy is generally twice as good. For smaller δ_a, ΔZ_a increases to 0.3 and 0.7 km for MERIS and POLDER, respectively. Indeed, the influence of aerosol scattering on the reflectance ratio is very weak in this case, and the method is more accurate for δ_a at 765 nm higher than 0.3.

Table 1 also indicates that an accurate specification of the spectral calibration of the MERIS absorbing channel improves the altitude retrievals. An uncertainty of 0.01 nm on the spectral position of the MERIS channel at 761.75 nm leads to a maximal deviation ΔZ_a of about 0.2 km for smaller δ_a and less than 0.1 km for larger δ_a. This accuracy is adequate for the aerosol altitude retrieval. Note that this spectral shift of ± 0.01 nm is on the order of the uncertainty on the in-flight spectral calibration of MERIS (Casadio & Colagrande, 2004; Dubuisson et al., 2003; Ramon et al., 2003). On the other hand, Table 1 shows that an uncertainty of 0.1 nm on the spectral calibration leads to much larger ΔZ_a values, and thus a precise spectral calibration is necessary to apply the differential absorption method to MERIS. To the contrary, the retrieved altitude Z_a with POLDER is less sensitive to the spectral calibration, due to the spectral definition of POLDER channels. Assuming the same spectral shifts, ΔZ_a is always less than 0.1 km.

Table 2 gives the accuracy of the method as a function of the surface reflectance at 765 nm, assuming a radiometric calibration of $\pm 0.5\%$ on R. As expected, the method is more efficient for dark surfaces. Indeed, for bright surfaces, outgoing photons are mainly coming from the surface and the contribution of the atmosphere to the TOA reflectance becomes negligible. In the case of dark surfaces, the contribution of the atmosphere to the TOA reflectance is predominant, due to scattering processes. The simulations reported in Table 2 show that the method is more accurate ($\Delta Z_a < 0.5$ km) for surface reflectance less than 0.06 with the POLDER instrument. Of course, considering $\Delta Z_a < 0.5$ km to be accurate is somewhat arbitrary. Due to its better sensitivity, the method can be applied to MERIS for relatively brighter surfaces in this case ($\Delta Z_a < 0.2$ km). Consequently, the applications to space measurements presented in Section 3 will be performed only over the open ocean, for which the surface reflectance at 765 nm is generally close to zero and spectrally neutral in the considered spectral range. However, high values of the marine reflectance can be observed over the ocean in the glitter pattern. According to the results of Table 2, the method will only be applied outside the glitter pattern. The glitter reflectance can be evaluated using the Cox and Munk model (1954), and reflectance thresholds can be defined for operational use. Note that over continental surfaces, the spectral dependence of the surface reflectance can be an additional source of uncertainty for the retrieval of aerosol altitude.

Table 3 displays the sensitivity of the method to uncertainties on the surface reflectance and aerosol model, as a function of δ_a at 765 nm. Reflectance simulations have been performed assuming realistic deviations on the surface reflectance ρ_s (± 0.005) and aerosol layer thickness H_a (± 0.5 km). In addition, three aerosol models (Dubovik et al., 2002), with various absorption and scattering properties at 765 nm, have been considered for simulations: oceanic ($\varpi_0 = 0.97$; $g = 0.68$), dust ($\varpi_0 = 0.96$; $g = 0.60$) and biomass burning ($\varpi_0 = 0.85$; $g = 0.56$). Table 3 shows that the sensitivity of the method to ρ_s or aerosol model is on the order of a few hundred meters for δ_a larger than 0.3. Knowledge of the surface reflectance and the aerosol model is then necessary for an accurate determination of Z_a. The aerosol layer thickness also contributes to retrieval quality, but to a lesser extent. Table 3 confirms that the retrievals are especially sensitive to aerosol properties or surface uncertainties for low aerosol optical thicknesses. In this case, ΔZ_a is ranging from 0.5 to 1 km for $\delta_a < 0.3$ and, consequently, the method will be more accurate for high δ_a. Note that the reflectance ratio R is also sensitive to the aerosol optical thickness (not shown). The aerosol optical thickness is a standard product for MERIS and POLDER, and it can therefore be used in the retrieval scheme. For clear atmospheres, the accuracy of this product can be estimated to 0.01 to 0.05 over marine or urban surfaces, respectively (Léon et al., 1999; Remer et al., 2005). Additional simulations have shown that an uncertainty of 0.05 on the aerosol

Table 1
Standard error ΔZ_a (km) on the retrieval of the altitude Z_a (from 1 to 6 km) of a 1 km aerosol layer assuming (a) a $\pm 0.5\%$ uncertainty on the ratio R due to the inter-band calibration or (b) an uncertainty on the spectral calibration with a spectral shift of ± 0.01 nm or ± 0.1 nm on the central wavelength of the O_2 channel of POLDER and MERIS.

ΔZ_a (km)						
	Inter-band calibration		Spectral calibration			
	$\pm 0.5\%$		± 0.1 nm		± 0.1 nm	
δ_a	POLDER	MERIS	POLDER	MERIS	POLDER	MERIS
0.1	0.7	0.3	0.1	0.2	0.1	1.2
0.2	0.4	0.2	<0.1	0.2	0.1	0.8
0.3	0.3	0.1	<0.1	0.1	<0.1	0.7
0.4	0.3	0.1	<0.1	0.1	<0.1	0.6
0.6	0.2	0.1	<0.1	<0.1	<0.1	0.5
1	0.2	0.1	<0.1	<0.1	<0.1	0.4

ΔZ_a is estimated from LUTs calculated with the GAME code (see section 2), as a function of the aerosol optical thickness δ_a at 765 nm, for various conditions of solar and view geometries (from 0 to 60°), with a surface reflectance of 0.01.

Table 2
Same as Table 1 but as a function of the surface reflectance ρ_s, assuming a $\pm 0.5\%$ uncertainty on the ratio R and with an aerosol optical thickness $\delta_a = 0.6$ at 765 nm.

ΔZ_a (km)		
ρ_s	POLDER	MERIS
0.01	0.2	0.1
0.02	0.3	0.2
0.04	0.4	0.2
0.06	0.5	0.2
0.1	0.6	0.3
0.2	0.7	0.4
0.3	0.9	0.6

Table 3
Sensitivity of the retrieved altitude Z_a obtained with POLDER reflectance ratio to the surface reflectance ρ_s, the aerosol model or the aerosol layer thickness H_a.

ΔZ_a (km)				
δ_a	$\Delta\rho_s = \pm 0.005$	Dust/oceanic	Dust/biomass	$\Delta H_a = \pm 0.5$ km
0.1	1.5 (1.5)	0.8 (0.8)	0.6 (0.6)	0.1 (0.1)
0.2	1 (0.9)	0.6 (0.6)	0.5 (0.5)	0.1 (0.1)
0.3	0.6 (0.6)	0.5 (0.5)	0.4 (0.4)	0.2 (0.1)
0.4	0.4 (0.4)	0.4 (0.4)	0.3 (0.3)	0.2 (0.1)
0.6	0.3 (0.2)	0.3 (0.3)	0.2 (0.2)	0.2 (0.2)
1	0.2 (0.2)	0.2 (0.2)	0.2 (0.2)	0.2 (0.2)

Results for MERIS are reported in parentheses. The standard error ΔZ_a (km) is calculated using the same conditions as in Table 1, assuming three aerosol models (Dubovik et al., 2002) with various absorbing properties: oceanic, dust and biomass burning. Sensitivity to the aerosol model is calculated (i) assuming the dust model in LUTs, and (ii) oceanic or biomass burning for reflectance ratio simulations as an input to the retrieval algorithm.

Table 4
Same as Table 3, but for the top-of-atmosphere reflectance ρ simulated in the non-absorbing channel (at 753 nm for MERIS, or 765 nm for POLDER).

$\Delta\rho$ (%)				
δ_a	$\Delta\rho_s = \pm 0.005$	Dust/oceanic	Dust/biomass	$\Delta H_a = \pm 0.5$ km
0.1	19	15	24	<1
0.2	15	23	39	<1
0.3	12	29	48	<1
0.4	10	32	53	<1
0.6	7	38	58	<1
1	5	40	59	<1

Standard error $\Delta\rho$ is expressed as relative difference (%).

optical thickness leads to a deviation of about 0.2 km or 0.1 km on Z_a for δ_a at 765 nm of 0.3 or 0.6, respectively. Such accuracy on the satellite product is acceptable for the proposed method.

In conclusion, the results presented in Tables 1–3 show that the reflectance ratio R is sensitive to aerosol altitude over marine surfaces, confirming the potential of using the oxygen absorption for aerosol altitude estimation. Nevertheless, an estimate of the aerosol altitude ($\Delta Z_a \leq 0.5$ km) requires knowing the surface reflectance and the optical aerosol properties (optical thickness and model). The accuracy of the aerosol optical thickness from MERIS or POLDER products is sufficient for the retrieval method. In addition, Table 4 shows the sensitivity of the reflectance in the non-absorbing channel to variations of the surface reflectance or aerosol properties. For convenience, the influence of these variations is expressed as relative difference (%). Table 4 shows that the reflectance in the non-absorbing channel is sensitive mainly to the surface reflectance and aerosol properties, and it is weakly affected by uncertainties on the aerosol layer thickness. As expected, the surface reflectance strongly impacts the TOA reflectance for smaller δ_a, while the aerosol model has an influence for all δ_a, and especially for δ_a larger than 0.3. However, the surface reflectance is not a critical parameter over ocean. Indeed, surface reflectance is generally close to zero, except in the glitter pattern or in coastal regions. As indicated above, in the glitter pattern the surface reflectance can be evaluated using the Cox and Munk (1954) parameterization, from the wind speed. By knowing the marine reflectance, the reflectance in the non-absorbing channel can then be used to constrain the choice of the aerosol model. This point is discussed in Section 3.1.

3. Application to POLDER and MERIS imagery over marine surfaces

3.1. Retrieval algorithm

Following the results of Section 2, a simple and fast algorithm for retrieval of aerosol altitude over the ocean from MERIS and POLDER instruments is presented in Fig. 3. The retrieval is based on measurements of the reflectance ratio R, which mainly depends on surface reflectance, aerosol optical properties, viewing and solar geometry. Some of these parameters are well known for each pixel in the satellite imagery, such as solar and viewing angles (θ_s, φ_s, θ_v, φ_v). The Rayleigh scattering and oxygen absorption can be accurately simulated from ancillary products, such as the surface pressure. Note that retrievals are performed using only clear pixels, selected from the cloud mask of MERIS or POLDER.

The aerosol optical thickness δ_a is available from satellite products at 865 nm for MERIS, and 670 nm and 865 nm for POLDER. However, the optical thickness δ_a at 765 nm is needed in the algorithm. The satellite products have been interpolated using the aerosol optical thickness and the Angström coefficient. In addition, Table 4 shows that the reflectance in the non-absorbing channel is mainly sensitive to the aerosol model, which can be evaluated from this reflectance. The most adequate aerosol model can be selected through comparisons between the simulated reflectance in the non-absorbing channel and measurements. For a given situation (solar and viewing angles, aerosol optical thickness, surface reflectance), the simulated reflectance is interpolated from LUTs for each aerosol model and compared with the satellite reflectance, in the non-absorbing channel. The best model is defined as the one that gives the lower difference between the simulated and satellite reflectance. The objective of this iterative procedure is not to determine the aerosol optical properties, but to improve the plume altitude retrieval by choosing the more appropriate aerosol model.

Finally, the reflectance in the absorbing and non-absorbing channels has been simulated for MERIS and POLDER, from their actual spectral response. The reflectance in the absorbing channel is

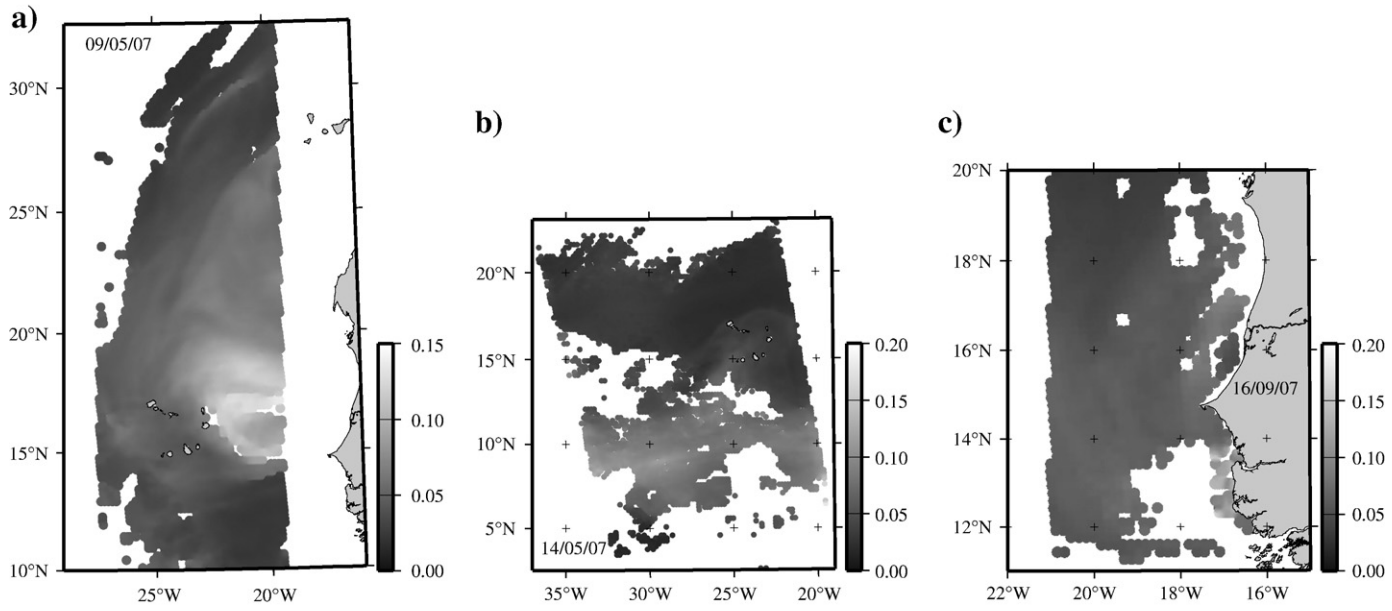

Fig. 4. Reflectances in the O_2 POLDER channel (763 nm) for the three scenes selected in Section 3.2, with aerosol plumes over Atlantic in May and September 2007.

very sensitive to the spectral calibration of the MERIS sensor (see Table 1). The LUTs have been calculated using the nominal spectral response and assuming a variable central wavelength in the range of ±1 nm, with a step of 0.01 nm to account for extreme shifts ('smile effect') observed during the spectral characterization before launch (Delwart et al., 2007; Dubuisson et al., 2003). The adequate LUT is then selected following the spectral shift given in the MERIS products, deduced from the in-flight calibration.

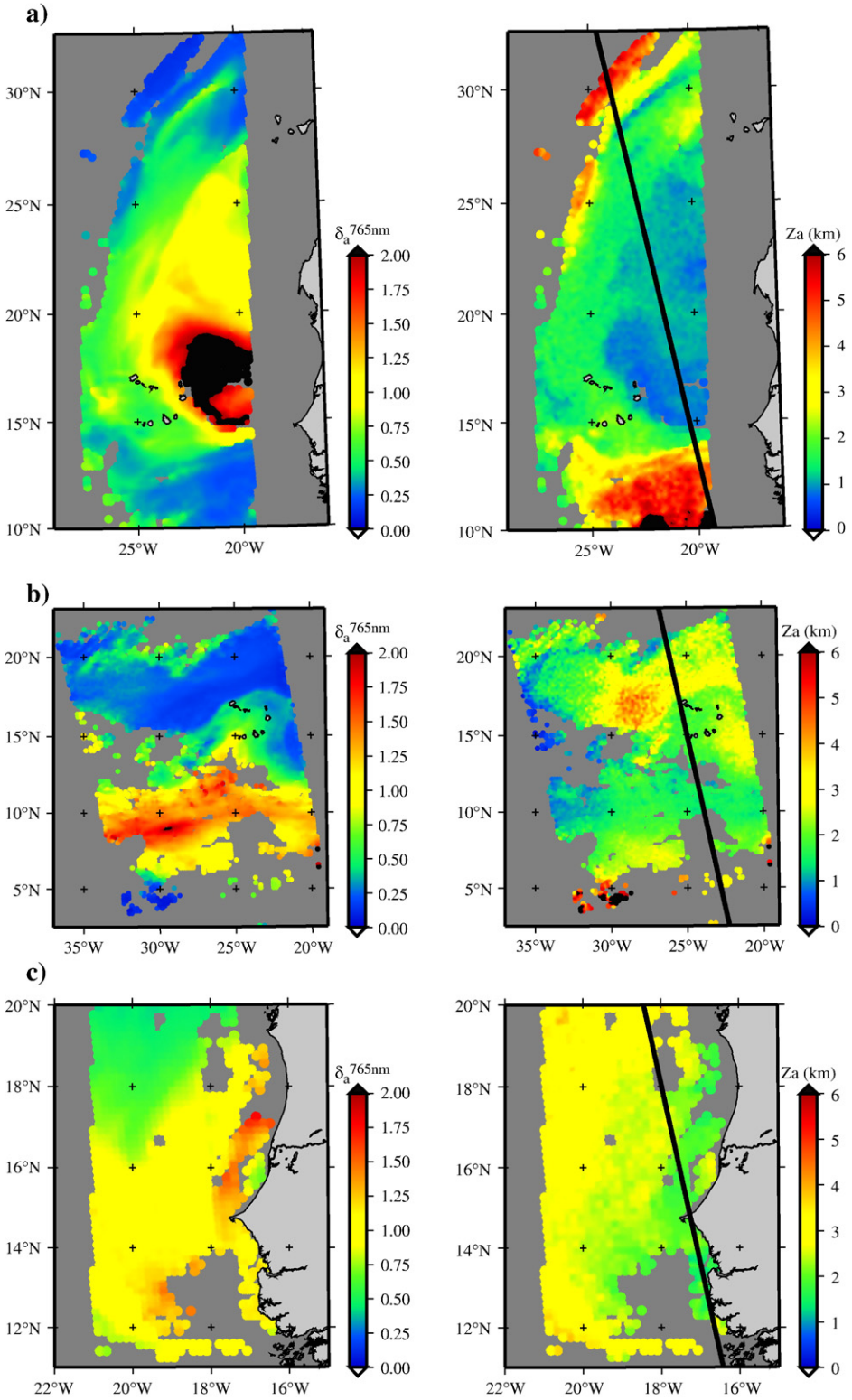

Fig. 5. Mean altitude Z_a (km) of a 1 km thick aerosol layer retrieved using the algorithm presented in Section 3.1 (right column), from the reflectance ratio measured with POLDER in the O_2 A-band for three reference scenes (see Fig. 4) showing dust plumes over the Atlantic. POLDER aerosol optical thickness product δ_a at 765 nm is also presented (left column). The CALIOP track is reported with the black solid line on the maps.

The methodology employs LUTs calculated with the GAME code. Relations between Z_a and R, presented in Fig. 2, have been developed for a wide range of parameters:

- Aerosol properties: optical thickness δ_a (0.02 to 3), layer altitude Z_a (0 to 10 km), layer thickness of 1 km and model (maritime, dust, urban, and biomass burning) defined by the single scattering albedo and asymmetry factor, and representative of absorbing or non-absorbing particles;
- Surface reflectance: ρ_s (0 to 0.1); the method is not applied if $\rho_s > 0.1$;
- Viewing and solar geometry: zenith angles θ_s, θ_v (0 to 80°) and azimuth angles φ_s, φ_v (0 to 180°).

From the measured reflectance ratio R, Z_a is obtained from the LUTs through interpolations. The estimated Z_a is defined as the median altitude of the aerosol layer.

Note that our goal was not to design an operational algorithm for MERIS and POLDER, but to have a simple algorithm to test the capabilities of the retrieval method from measurements. Some peculiarities of MERIS or POLDER have not been included in our inversion scheme. For example, the degree of linear polarization inside the O_2 A-band is sensitive to aerosol altitude (Boesche et al., 2008). These authors have also shown a high sensitivity of the degree of polarization to microphysical properties and optical thickness of aerosol. This aspect is not presented in this study, because the POLDER and MERIS channels in the O_2 A-band are not polarized. However, polarization of the skylight in the O_2 A-band would be certainly useful to improve the aerosol altitude inversion. Furthermore, we have used realistic but arbitrary aerosol models for LUTs calculations. Using the same aerosol models than those in the POLDER or MERIS operational algorithm to estimate the aerosol optical thickness product would improve the inversion or, at least, the coherence of the inversion scheme.

3.2. Results using POLDER data

The methodology described in the previous section has been applied to POLDER data. Spectral characteristics of the POLDER instrument, onboard PARASOL, allow an estimate of the apparent pressure in the oxygen band (Buriez et al., 1997; Vanbauce et al., 1998). Moreover, POLDER has the ability to measure directional characteristics of the light reflected by a given pixel. The aerosol altitude can then be estimated for the same pixel using several view angles (up to 16 directions). In addition, simultaneous measurements of the space-borne lidar CALIOP can be used for comparison purposes (both instruments are onboard satellites of the A-train constellation). CALIOP is a three-channel backscatter lidar aboard CALIPSO, optimized for aerosol and cloud profiling and operating in the nadir view (Winker et al., 2004). CALIOP provides information on the vertical distribution of atmospheric particles, allowing direct comparisons with POLDER estimates.

Three scenes have been selected with optimal conditions for comparisons, i.e., with cloudless atmosphere and high aerosol loading (Fig. 4). For these scenes, simultaneous data from POLDER and CALIOP are available. Fig. 5 presents the POLDER aerosol optical thickness products for the selected scenes, with aerosol plumes over Atlantic in May and September 2007. Retrieved altitude Z_a obtained with the algorithm described in Section 3.1 is also presented in Fig. 5 for the three scenes. Altitudes in Fig. 5 are the average altitudes over all POLDER directions. Fig. 5 reveals a coherent spatial distribution for retrieved altitude Z_a. In the case of large δ_a, aerosols are mainly located between 1 and 3 km, a typical situation for dust aerosols over the western coast of Africa. For small δ_a, the theoretical study has shown that the method is not adapted, and accordingly the method overestimates the aerosol altitude. Indeed, the POLDER reflectance ratio is higher for low optical thickness δ_a. According to the simulations, these high reflectance ratios can only correspond to (1) a single aerosol layer at an altitude Z_a of around 4 to 6 km or (2) aerosols vertically distributed with a scale height of about 4 to 6 km. These results show that the influence of scatterers located at higher altitudes is not negligible in this case and the method is not adapted for lower δ_a.

The POLDER capability to observe a surface point from multiple view angles has been also exploited. The variability ΔZ_a of the retrieved altitude has been evaluated from POLDER measurements. ΔZ_a is defined as the root mean square altitude error, calculated from altitudes retrieved for the 16 viewing directions available with POLDER for a same pixel. Fig. 6 presents the standard deviation of ΔZ_a as a function of the aerosol optical thickness δ_a at 765 nm, for all pixels of the previous scenes. The standard deviation ΔZ_a allows an estimate of the method accuracy, i.e., ΔZ_a is on the order of 0.1 km for large δ_a, with a small variability represented with vertical error bars in Fig. 6. This accuracy decreases to about 0.6 km for low aerosol amounts, with a larger dispersion. Fig. 6 confirms that the method is more accurate for δ_a larger than 0.3 with POLDER. These results are coherent with theoretical estimates presented as a function of the aerosol optical thickness in Table 1.

Comparisons between POLDER estimates (mean altitude of a 1 km aerosol layer) and CALIOP measurements (top and bottom of the aerosol layer), for May 9, are presented in Fig. 7. These comparisons show agreement to within 0.5 km with the CALIOP retrieval of the median altitude of the aerosol layer (level-2 data product), for latitudes ranging from 14° to 26° on the CALIPSO track. This deviation can be explained by uncertainties on the aerosol properties used in the retrieval algorithm (optical thickness and model) or inhomogeneous vertical distribution of aerosol particles in the layer. However, for latitude ranging from 12° to 14°, the aerosol optical thickness is less than 0.4 and once again, the retrieved altitude is overestimated ($Z_a \geq 4$ km). Note that there is no altitude information from CALIOP in this case, δ_a being too small. On May 14 (Fig. 8), comparisons agree for higher latitudes (13° to 17°) with small differences. Deviations increase up to 1 km for latitude between 7° and 13°, with δ_a at 765 nm larger than 0.5. The aerosol altitude Z_a is underestimated and simulations have shown that these deviations can only be explained with the presence of a more complex vertical structure for aerosols, including a layer near the surface, or by the presence of low clouds

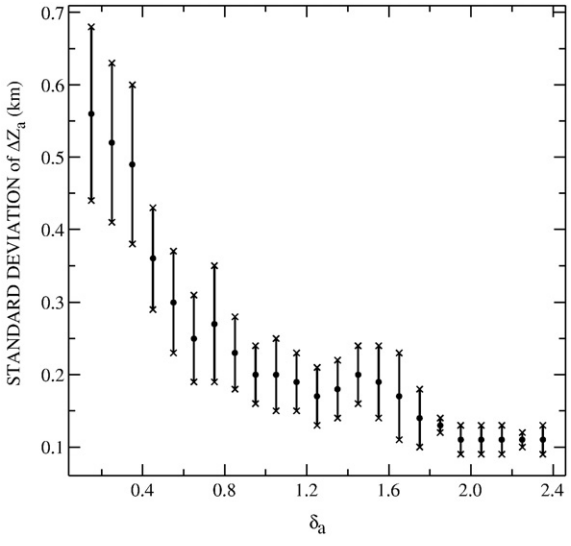

Fig. 6. Standard deviation of ΔZ_a (dots) as a function of the aerosol optical thickness δ_a at 765 nm for the three reference scenes presented in Fig. 5. ΔZ_a is defined as the root mean square deviation calculated from altitudes Z_a (km) retrieved for the 16 viewing directions available for a pixel observed with POLDER. The standard deviation of ΔZ_a has been calculated for all pixels along the CALIOP track and averaged over 0.1 optical thickness bin. The variability (root mean square) on ΔZ_a is reported with vertical error bars.

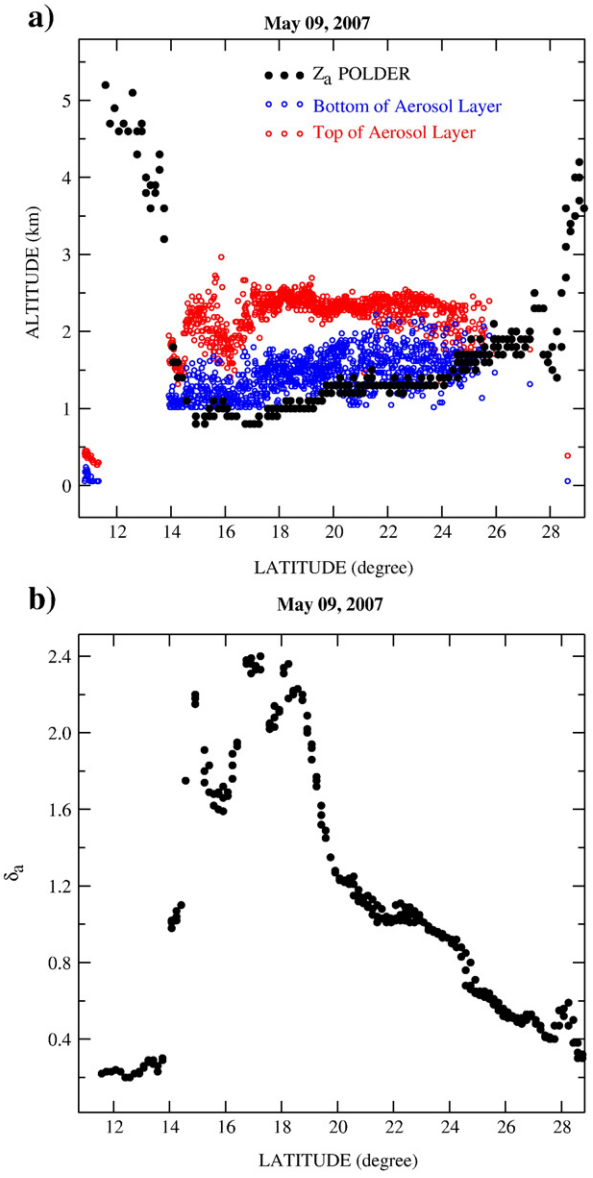

Fig. 7. Comparisons (upper curve) between the altitude of the top (red circles) and bottom (blue circles) of the aerosol layer obtained from CALIOP level-2 products, and the altitude Z_a retrieved using POLDER reflectance ratio measurements (black circles). Comparisons are presented as a function of the latitude, along the CALIOP track and for the reference scene on May 09, 2007 (see Fig. 5). Z_a is defined as the mean altitude of 1 km thick aerosol layer. The aerosol optical thickness δ_a at 765 nm, obtained from POLDER products and used in the retrieval algorithm, is reported as a function of the latitude (lower curve). (For interpretation of the references to colour in this figure legend, the reader is referred to the web version of this article.)

located under the aerosol layer. This situation seems possible since CALIOP measurements show the presence of a second layer, especially for latitudes ranging from 12° to 13°. Conclusions are quite similar for comparisons on September 16 (Fig. 8), with coherent retrievals with POLDER as a function of the vertical distribution of aerosols.

3.3. Results using MERIS data during AOPEX

Comparisons between *in situ* measurements of the aerosol vertical distribution and retrieved altitudes from MERIS data using the algorithm described in Section 3.1 have been also performed. Measurements collected at sea during the Advanced Optical Properties EXperiment (AOPEX) 2004 (Antoine et al., 2006) in July–August 2004 over the western Mediterranean Sea have been used, as well as MERIS observations available during the campaign (Fig. 9). Nearly simultaneous *in situ* lidar data have been also obtained. These lidar data have been processed into profiles of backscattering coefficients according to Voss et al. (2001) and Welton and Campbell (2002). Aerosol optical thickness derived from MERIS data is available to apply the oxygen absorption method, as well as *in situ* measurements from five sun photometers. Validations of the MERIS aerosol optical thickness product, performed in previous studies through comparisons with *in situ* measurements, have shown a good correlation with MERIS slightly underestimating the aerosol optical thickness (Bécu et al., 2003; Ruddick et al., 2003). Surface pressure measurements are also available. The four study cases presented in Table 5 have been analyzed. These cases correspond to the situations observed during AOPEX with clear atmospheric conditions and outside the glitter pattern (ρ_s<0.1). Uncertainties on *in situ* aerosol optical thickness

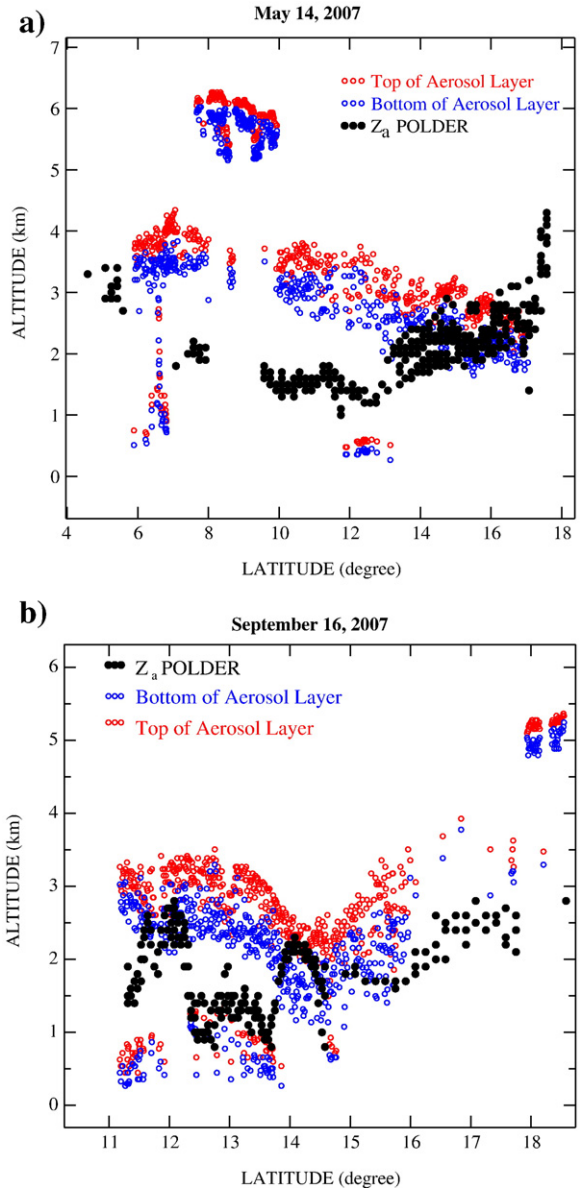

Fig. 8. Comparisons between the altitude of the top (red circles) and bottom (blue circles) of the aerosol layer obtained from CALIOP level-2 products, and the altitude Z_a retrieved using POLDER reflectance ratio measurements (black circles). Comparisons are presented as a function of the latitude, along the CALIOP track and for the reference scenes on May 14 and September 16, 2007 (see Fig. 5). Z_a is defined as the mean altitude of 1 km thick aerosol layer. Note that CALIOP data indicate the presence of high clouds between 5 and 6 km. (For interpretation of the references to colour in this figure legend, the reader is referred to the web version of this article.)

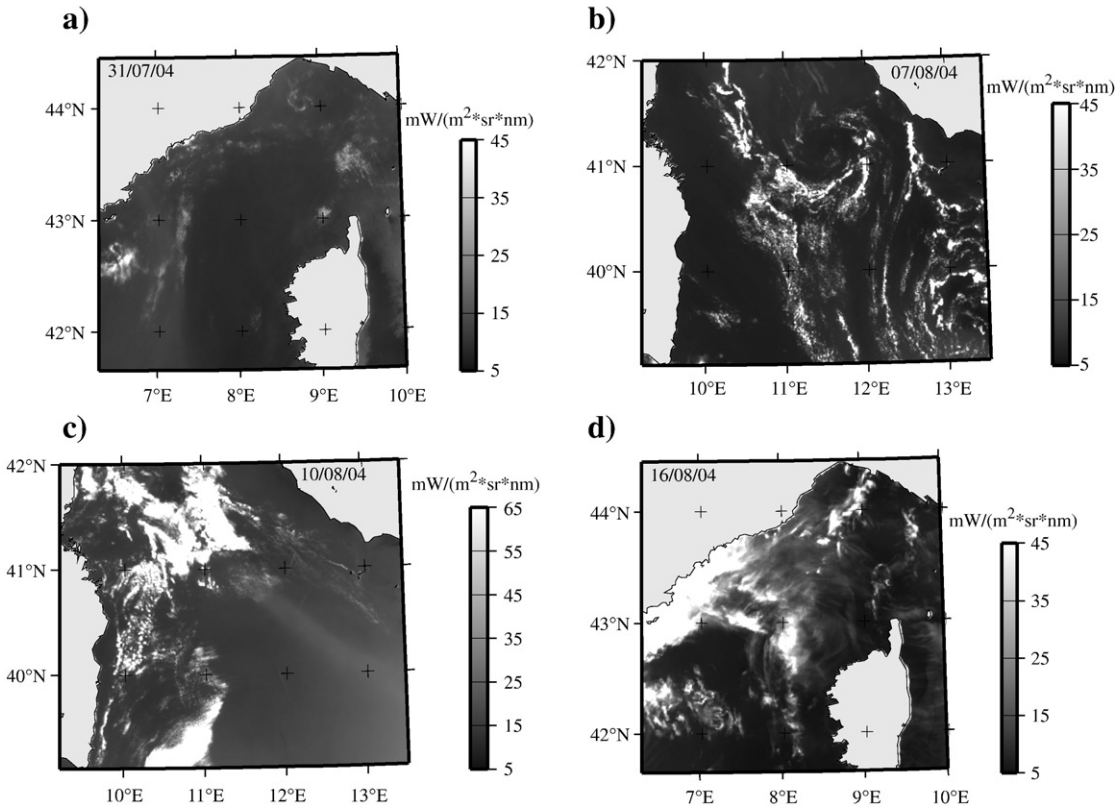

Fig. 9. Normalized radiances in the O_2 MERIS channel (761.75 nm) for the four situations presented in Table 5 over the AOPEX campaign area during summer 2004.

have been estimated using simultaneous measurements obtained from the five sun photometers. These uncertainties are reported in Table 5 and indicate that the measurements agree with the MERIS products. In addition, a situation including high and thin cirrus clouds has been added to complete the analysis.

Fig. 10 presents the retrievals for the four scenes. The MERIS aerosol product is presented over the AOPEX region. The retrieved aerosol altitude, obtained with our algorithm, is presented for the same area using aerosol optical thickness from MERIS products. Low aerosol layers ($0\ \text{km}<Z_a<1\ \text{km}$) are generally obtained, except on August 16 ($Z_a>5$ km) suggesting the presence of optically thin high clouds. Profiles of backscattering coefficient, as well as altitude estimates calculated using δ_a from MERIS, are also reported in Fig. 11 for the measurement stations (represented in Fig. 10 with the symbol ♦ on the map). Fig. 11 compares the relevant lidar profiles with the algorithm derived aerosol altitude, for the three scenes with clear atmospheric conditions and the scene with upper level cirrus clouds. Note that δ_a at 765 nm from MERIS products is less than 0.3 for the three clear scenes. These low aerosol loadings do not provide optimal conditions for testing of the method. On August 7, 2004, using the aerosol optical depth from MERIS ($\delta_a=0.1$) results in an aerosol height lower than the one found in the lidar profiles. Considering the uncertainties of *in situ* measurements of δ_a reported in Table 5, the retrieved altitude (presented as a vertical error bar in Fig. 11) is coherent with the lidar vertical profile. On August 10, the method provides satisfactory estimates in the case of a single and homogeneous aerosol layer and using the δ_a obtained from MERIS products. This situation substantiates that a satisfactory accuracy (about 0.1 km) can be reached for larger δ_a. These comparisons confirm that it is possible to estimate the aerosol altitude for a single aerosol layer if the optical thickness δ_a is known, even in the case of small optical thicknesses ($\delta_a<0.3$) due to the better sensitivity of MERIS (see Section 2). However, the retrieval is very sensitive to δ_a in this case, with larger uncertainties on August 10, 2004 ($\delta_a=0.1$ in Fig. 11), and a correct estimate of δ_a is then needed. On July 31, 2004, in the case of a multilayer structure, the algorithm also does a good job of finding the top of the aerosol layer with MERIS data or *in situ* measurements. Finally, the method is highly sensitive to the presence of cirrus clouds. On august 16, 2004, a cirrus cloud is present near 10 km height. The cloud strongly influences the reflectance ratio and the retrieved aerosol altitude is much higher than the actual one. This is evidenced in Fig. 10, which exhibits a large number of pixels with too high altitude. The presence of thin cirrus is sensed, but incorrectly interpreted as aerosol with the MERIS product. This suggests that the method may be used to detect thin clouds in satellite imagery and, consequently, to improve cloud screening algorithms.

Table 5
Situations available during the AOPEX experiment for the validation of retrieved aerosol altitude.

Date	MERIS δ_a	*In situ* δ_a	
31 July 2004	0.20 at 9H55	0.19 ± 0.02	Clear atmosphere with aerosols
7 August 2004	0.11 at 9H35	0.11 ± 0.02	
10 August 2004	0.30 at 9H41	0.29 ± 0.01	
16 August 2004	Not available	Not available	Cirrus clouds

Aerosol optical thicknesses δ_a at 765 nm, obtained from MERIS products, and acquisition time are reported. *In situ* measurements of δ_a, obtained from five different ground-based sun photometers during the acquisition time of MERIS, are also presented. The uncertainties on δ_a have been evaluated from the measurements of the five photometers.

4. Conclusions

A method has been presented for estimating the altitude of aerosol plumes over the ocean from space. The method is based on reflectance ratio measurements in the spectral region of the O_2 A-band. The altitude of an aerosol layer is related, through simple parameterizations, to the reflectance ratio defined as the ratio of the reflectance

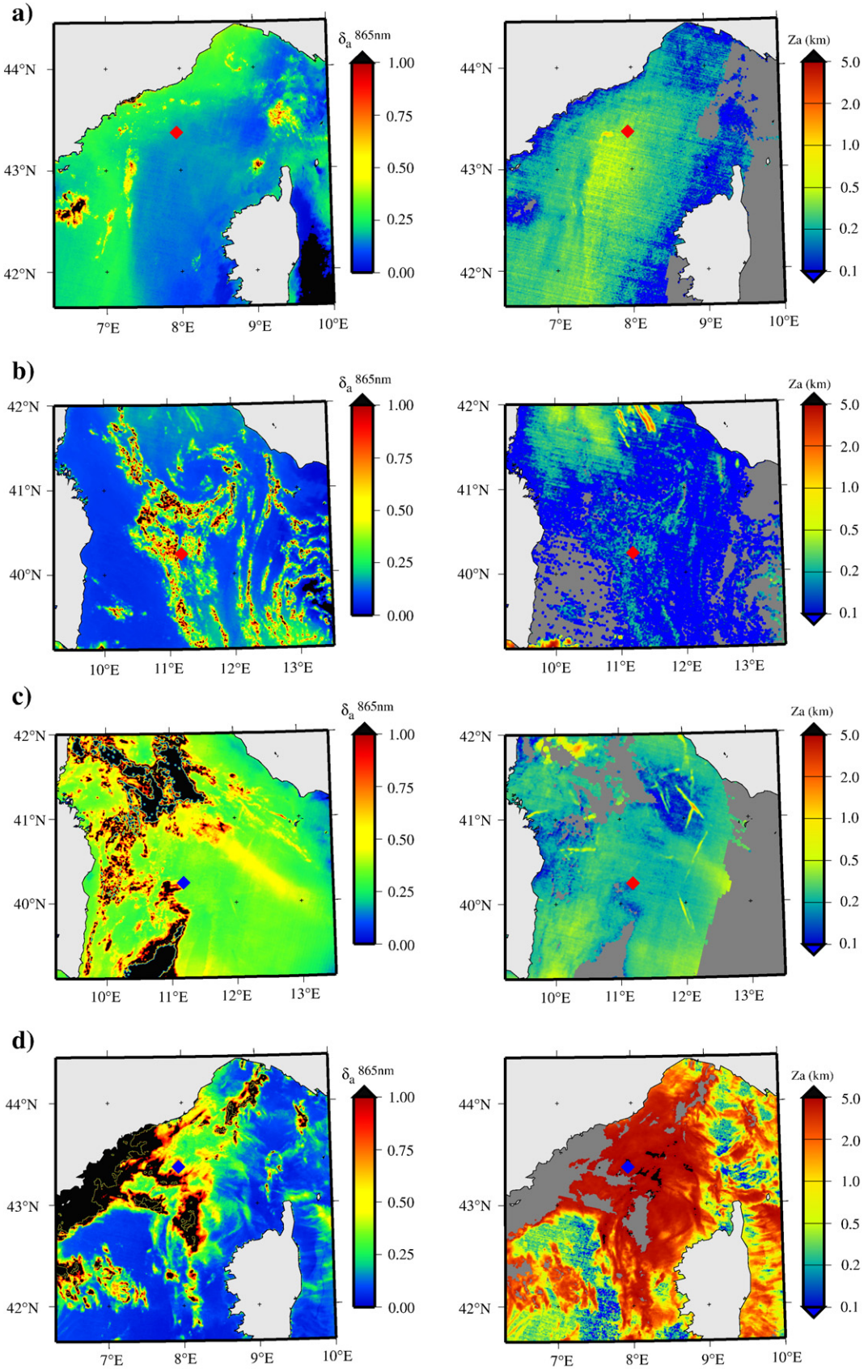

Fig. 10. MERIS aerosol product δ_a at 865 nm (left column) and retrieved aerosol altitude Z_a (right column) over the AOPEX campaign area during summer 2004, for the four situations presented in Table 5 and Fig. 9. Aerosol altitude is estimated from MERIS reflectance ratio, using δ_a from MERIS products. The station localization (with lidar *in situ* measurements) is represented with the symbol ♦ on the maps.

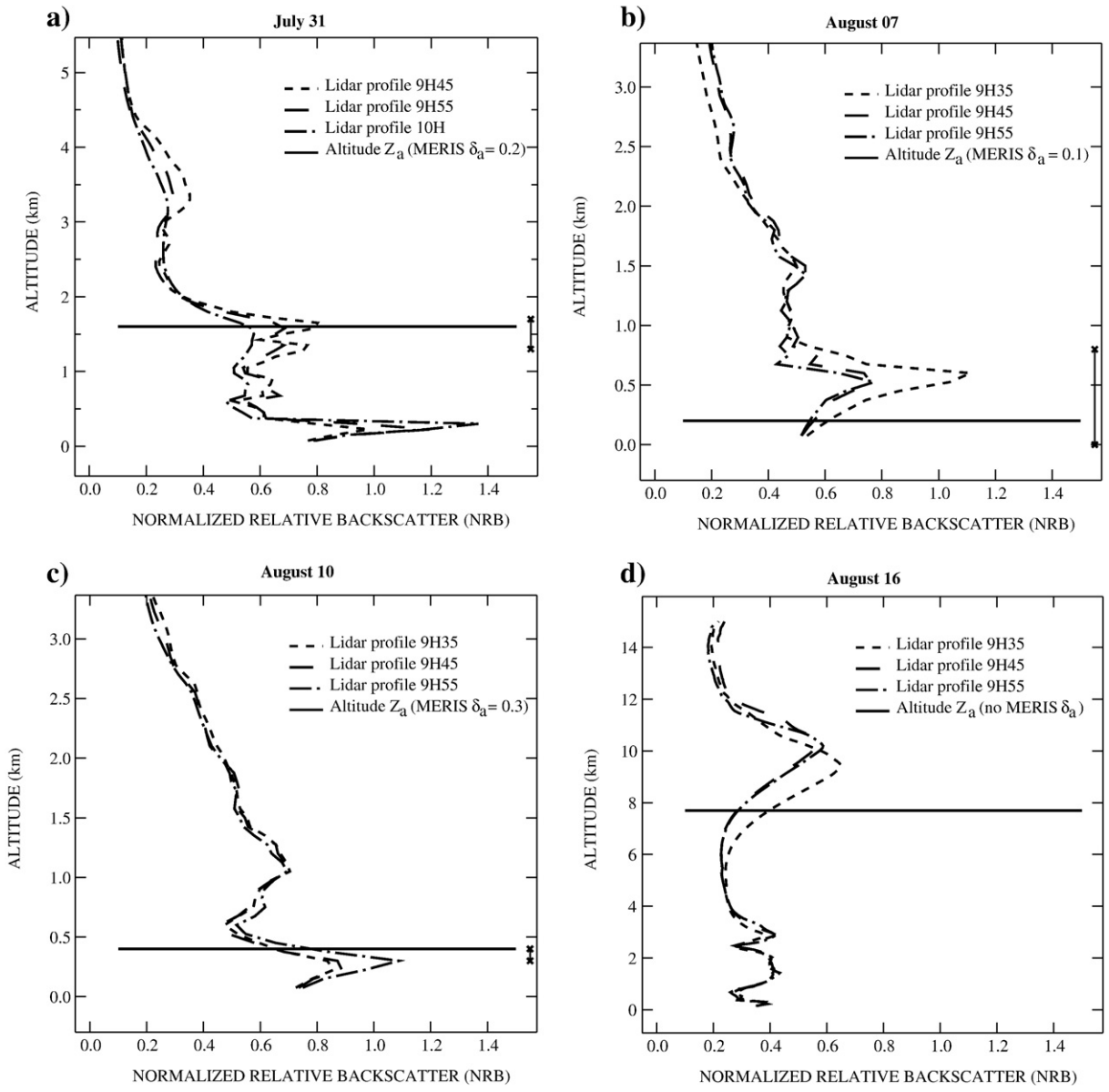

Fig. 11. *In situ* lidar profiles of backscattering coefficient (dashed lines) at the measurement stations, measured during the AOPEX campaign for the four stations represented with the symbol ♦ on the maps in Fig. 10. Aerosol altitude Z_a, estimated from MERIS reflectance ratio and δ_a MERIS products, is represented with horizontal solid lines. In addition, the vertical error bar represents the extreme altitudes calculated using *in situ* δ_a uncertainty obtained from ground-based measurements (see Table 5).

measured in an absorbing channel and in a close non-absorbing channel. Parameterizations are compiled into LUTs to provide a fast and simple algorithm. The parameterizations have been obtained using the high spectral resolution radiative transfer code GAME. The LUTs have been calculated for the space sensors MERIS and POLDER, which have adequate spectral characteristics. A theoretical analysis has shown an expected accuracy of about of ± 0.5 km or ± 0.2 km for POLDER or MERIS, respectively. This theoretical accuracy can be reached for higher aerosol optical thickness ($\delta_a > 0.3$), over dark surfaces ($\rho_s < 0.06$), and assuming a calibration accuracy of $\pm 0.5\%$ on the reflectance ratio. More accurate estimates are obtained with MERIS, because the 754 nm band is outside the oxygen absorption lines. However, a precise spectral calibration is needed for MERIS. It is important to notice that the method is only accurate ($\Delta Z_a < 0.5$ km) for a surface reflectance less than 0.06 with POLDER measurements. The POLDER spectral characteristics restrict the field of application, limiting the method to marine surfaces. Due to its better sensitivity, the method could be applied to MERIS for relatively brighter surfaces, at least in theory.

The methodology has been applied to MERIS and POLDER (onboard PARASOL) imagery over marine surfaces, with coherent results with respect to the theory and measurements. Retrieved altitudes have been compared with *in situ* profiles of backscattering coefficient acquired during the AOPEX 2004 experiment for MERIS, or with CALIOP measurements in the context of the A-train for POLDER. Coherent altitudes have been obtained for the available situations. The retrieved method is sensitive to the vertical distribution of scatterers allowing an estimation of the altitude of the aerosol layer with an accuracy on the order of 0.5 km. Comparisons have confirmed that the method is only accurate for aerosol optical thicknesses larger than 0.3 at 765 nm, but the lidar comparisons show fairly good agreement with MERIS derived altitudes for lower δ_a values. Indeed, the spectral definition of channels in the O_2 A-band leads to a better sensitivity to altitude with MERIS than POLDER. In addition, cirrus clouds have a strong impact on the retrievals. Comparisons between MERIS data and aerosol altitude retrievals have shown that the method provides information on the presence of cirrus clouds making it possible to detect thin high clouds for pixels defined as clear in operational

algorithms. All results demonstrate the potential of the differential absorption methodology for obtaining information on the altitude of an aerosol layer. Using this information in atmospheric correction algorithms may improve the retrieval of marine reflectance in the presence of aerosols or thin cirrus clouds (Duforêt et al., 2007). In addition, knowledge of the aerosol altitude may be used to improve the retrievals of microphysical and optical properties of absorbing aerosols and calculations of aerosol radiative forcing, especially indirect forcing.

The proposed methodology is based on simple parameterizations and LUTs and can then be easily applied operationally to current sensors such as POLDER or MERIS. However, the use of a two-band technique limits the potential of the method and only one piece of information is reachable. For example, additional tests have shown that the retrieved plume altitudes are quite similar if the vertical distribution of aerosols varies exponentially with altitude in the LUTs, with a scale height, instead of having the aerosols concentrated in a single layer. In the case of complex vertical structures such as a multilayer system, only the mean altitude of particles in the total atmospheric column is available. Potential of the degree of linear polarization inside the O_2 A-band for estimating the altitude of a single aerosol layer has been demonstrated, but limitations exist in the case of multiple aerosol layers (Boesche et al., 2008). Accurate retrievals of aerosol vertical distribution would be possible from radiometric measurements only if more information is available. This may be achieved with additional spectral bands or angular observations (Frouin et al., 2007) and using the polarization of skylight in the oxygen A-band. Koppers et al. (1997) have also demonstrated that a complete description of aerosol properties is possible from high spectral resolution measurements in the Oxygen A-band, at least in theory. More recently, Pelletier et al. (2007, 2008) proposed a methodology to retrieve the vertical distribution of aerosol from multi-angular measurements in the oxygen A-band, using a spectral resolution comparable to the MERIS one. Although the method, which seeks regularization solutions, is more complex than a simple two-band ratio technique, it is applicable to space sensors such as POLDER-PARASOL, or ground-based instruments such as AERONET sky radiometers (Holben et al., 1998). Indeed, these instruments offer the possibility to measure reflectance in multi-angular conditions. The above approaches constitute interesting alternatives to lidar systems, offering the opportunity to provide information on aerosol vertical structure, not only at nadir, but over the entire swath of satellite sensors.

Acknowledgments

This work was supported by the “Centre National d'Etudes Spatiales” (CNES), the “Conseil Régional du Nord-Pas-de-Calais” and the “Programme National de Télédétection Spatiale” (PNTS). The BOUSSOLE project, within which the AOPEX cruise was organized, was set up by numerous people with funding from several Agencies and Institutions, whose support is gratefully acknowledged. Specifically, the following contracts are acknowledged: CNES (the French space Agency) provided funds through the TAOB and TOSCA scientific committees, ESA through ESTEC contract 14393/00/NL/DC and through ESRIN contract 17286/03/I-OL. NASA provided support through a Letter of Agreement. Funding has been also obtained from the French CSOA (INSU) committee and the Observatoire Océnologique de Villefranche. The “Institut National des Sciences de l'Univers” (INSU) provides ship time for the monthly cruises. IFREMER provided ship time for the AOPEX cruise (R/V “Le Suroît”). The crews and captains of the INSU R/V “Téthys-II” and IFREMER “Le Suroit” are warmly thanked for their help at sea. The lidar data was collected with support of NASA under contract NG04HZ21C by the late Albert Chapin. The participation of Robert Frouin in the AOPEX cruise was supported by NASA under contract no. NNX08AF65A and by the Scripps Institution of Oceanography, University of California at San Diego.

References

Antoine, D., Chami, M., Claustre, H., D'Ortenzio, F., Morel, A., Bécu, G., et al. (2006). BOUSSOLE: A joint CNRS-INSU, ESA, CNES and NASA ocean color calibration and validation activity. NASA technical memorandum, N° TM-2006-214147, NASA/GSFC, Greenbelt, USA.

Al-Saadi, J., Szykman, J., Pierce, R. B., Kittaka, C., Neil, D., Chu, D. A., et al. (2005). Improving national air quality forecasts with satellite aerosol observations. *Bulletin of the American Meteorological Society*, *86*(9), 1249—1261.

Badayev, V. V., & Malkevich, M. S. (1978). On the possibility of determining the vertical profiles of aerosol attenuation using satellite measurements of reflected radiation in the 0.76-mm oxygen band. Izv. *Atmospheric and Oceanic Physics*, *14*, 722—727.

Barton, I. J., & Scott, J. C. (1986). Remote measurement of surface pressure using absorption in the oxygen A-band. *Applied Optics*, *25*, 3502—3507.

Bécu, G., Deschamps, P. -Y., & Nicolas, J. -M. (2003). MERIS level-2 products validation using SIMBADA radiometer network. *Proceedings of Envisat Validation Workshop 2002* ESA SP-531.

Boesche, E., Stammes, P., Preusker, R., Bennartz, R., Knap, W. H., & Fischer, J. (2008). Polarization of skylight in the O2A-band: Effects of aerosol properties. *Applied Optics*, *47*(19), 3467—3480. doi:10.1364/AO.47.003467

Boucher, O. (2002). *Aerosol radiative forcing and related feedbacks: How to reduce uncertainties?* (pp. 8—12). IGAC-tivities.

Bréon, F. M., & Bouffiès, S. (1996). Land surface pressure estimates from measurements in the oxygen A absorption band. *Journal of Applied Meteorology*, *35*, 69—77.

Brogniez, C., Bazureau, A., Lenoble, J., & Chu, W. P. (2002). SAGE III measurements: A study on the retrieval of ozone, nitrogen dioxide and aerosol extinction coefficients. *Journal of Geophysical Research*, *107*, D24. doi:10.1029/2001JD001576

Buriez, J. -C., Vanbauce, C., Parol, F., Goloub, P., Herman, M., Bonnel, B., et al. (1997). Cloud detection and derivation of cloud properties from POLDER. *International Journal of Remote Sensing*, *18*, 2785—2813.

Casadio, S., & Colagrande, P. (2004). MERIS O2 calibration using SCIAMACHY measurements. In H. Lacoste (Ed.), *Proceedings of MERIS User Workshop (ESA SP-549). 10–13 November 2003, ESA-ESRIN, Frascati, Italy*.

Chance, K. V. (1997). Improvement of the O2-A-band spectroscopic database for satellite-based cloud detection. *Journal of Quantitative Spectroscopy & Radiative Transfer*, *58*(3), 375—378.

Cox, C., & Munk, W. (1954). Measurements of the roughness of the sea surface from photographs of the sun's glitter. *Journal of the Optical Society of America*, *44*, 838—850.

DeHaan, J. F., Bosma, P. B., & Hovenier, J. W. (1987). The adding method for multiple scattering calculations of polarized light. *Astronomy & Astrophysics*, *183*, 371—391.

Delwart, S., Preusker, R., Bourg, L., Santer, R., Ramon, D., & Fischer, J. (2007). MERIS in flight calibration. *International Journal of Remote Sensing*, *28*, 479—496. doi:10.1080/01431160600821119

Deschamps, P. Y., Bréon, F. M., Leroy, M., Podaire, A., Bricaud, A., Buriez, J. C., et al. (1994). The POLDER mission: Instrument characteristics and scientific objectives. *IEEE Transactions on Geoscience and Remote Sensing*, *32*, 1398—1411.

Dubovik, O., Holben, B. N., Eck, T. N., Smirnov, A., Kaufman, Y. J., King, M. D., et al. (2002). Variability of absorption and optical properties of key aerosol types observed in worldwide locations. *Journal of the Atmospheric Sciences*, *59*, 590—608.

Dubuisson, P., Borde, R., Dessailly, D., & Santer, R. (2003). In-flight spectral calibration of the oxygen A-band channel of MERIS. *International Journal of Remote Sensing*, *24*(5), 1177—1182.

Dubuisson, P., Borde, R., Schmechtig, C., & Santer, R. (2001). Surface pressure estimates from satellite data in the oxygen A-band: Applications to the MOS sensor over land. *Journal of Geophysical Research*, *106*(D21), 27,277—27,286.

Dubuisson, P., Buriez, J. C., & Fouquart, Y. (1996). High spectral resolution solar radiative transfer in absorbing and scattering media, application to the satellite simulation. *Journal of Quantitative Spectroscopy & Radiative Transfer*, *55*, 103—126.

Duforêt, L., Frouin, R., & Dubuisson, P. (2007). Importance and estimation of aerosol vertical structure in satellite ocean-colour remote sensing. *Applied Optics*, *46*, 1107—1119.

Dufresne, J. -L., Gautier, C., Ricchiazzi, P., & Fouquart, Y. (2002). Longwave scattering effects of mineral aerosols. *Journal of the Atmospheric Sciences*, *59*, 1959—1966.

Fischer, J., & Grassl, H. (1991). Detection of cloud-top height from backscattered radiances within the oxygen A-band. Part. I: Theoretical study. *Journal of Applied Meteorology*, *10*, 1245—1259.

Frouin, R., Pierre-Yves Deschamps, P. -Y., Rotschchild, R., Stephan, E., Leblanc, P., Duttweiler, F., et al. (2007). MAUVE/SWIPE: An imaging instrument concept with multi-angular, -spectral, and -polarized capability for remote sensing of aerosols, ocean color, clouds, and vegetation from space. In R. Frouin, V. J. Argaway, H. Kawamura, & D. Pan (Eds.), *Remote sensing of the marine environmentProceedings of SPIE, Vol. 6406*. (pp.). doi:10.1117/12.698061

Gabella, M., Guzzi, R., Kisselev, V., & Perona, G. (1997). Retrieval of aerosol pro le variations in the visible and near infrared: Theory and application of the single scattering approach. *Applied Optics*, *36*, 1328—1336.

Gabella, M., Kisselev, V., & Perona, G. (1999). Retrieval of aerosol profile variations from reflected radiation in the oxygen absorption A-band. *Applied Optics*, *39*, 3190—3195.

Gordon, H. R. (1997). Atmospheric correction of ocean color imagery in the Earth Observing System era. *Journal of Geophysical Research*, *102*, 17,107—17,118.

Gordon, H. R., Zhang, T., He, F., & Ding, K. (1997). Effects of stratospheric aerosols and thin cirrus clouds on atmospheric correction of ocean color imagery: Simulations. *Applied Optics*, *36*, 682—697.

Hagolle, O., Goloub, P., Deschamps, P. -Y., Cosnefroy, H., Briottet, X., Bailleul, T., et al. (1999). Results of POLDER in-flight calibration. *IEEE Transactions on Geoscience and Remote Sensing*, *37*(3), 1550—1566.

Holben, B. N., Eck, T. F., Slutsker, I., Tanre, D., Buis, J. P., Setzer, A., et al. (1998). AERONET — A federated instrument network and data archive for aerosol characterization. *Remote Sensing of Environment*, *66*, 1—16.

Koppers, G. A. A., Murtagh, D. P., & Jansson, J. (1997). Aerosol optical thickness retrieval from GOME data in the oxygen A-band. *Proceedings of the Third ERS Symposium, Florence, Italy (1997)* (pp. 693−696).

Léon, J. F., Chazette, P., & Dulac, F. (1999). Retrieval and monitoring of aerosol optical thickness over an urban area by spaceborne and ground-based remote sensing. *Applied Optics*, *38*, 6918−6926.

Liao, H., & Seinfeld, J. H. (1998). Radiative forcing by mineral dust aerosols: Sensitivity to key variables. *Journal of Geophysical Research*, *103*, 31,637−31,645.

Pelletier, B., Frouin, R., & Dubuisson, P. (2007). Maximum entropy regularization strategies for inferring aerosol vertical distribution from light scattering measurements. In R. Frouin, V. J. Argaway, H. Kawamura, & D. Pan (Eds.), *Remote sensing of the marine environmentProceedings of SPIE*, *Vol. 6406*. doi:10.1117/12.738168

Pelletier, B., Frouin, R., and Dubuisson, P. (2008). Retrieval of the aerosol vertical distribution from atmospheric radiance. In remote sensing of inland, coastal, and oceanic waters, R. Frouin, S. Andrefouet, H. Kawamura, M.J. Lynch, D. Pan, and T. Platt, Eds., Proceedings of SPIE 7150, 9 pp., in press.

Ramon, D., Cazier, L., & Santer, R. (2003). The surface pressure retrieval in the MERIS O2 absorption: Validation and potential improvements. *Geoscience and Remote Sensing Symposium, IGARSS'03IEEE International Publication*, *Vol. 5*. (pp. 3126−3128).

Rast, M., Bézy, J. L., & Bruzzi, S. (1999). The ESA medium resolution imaging spectrometer MERIS: A review of the instrument and its mission. *International Journal of Remote Sensing*, *20*, 1681−1702.

Remer, L. A., Kaufman, Y. J., Tanré, D., Mattoo, S., Chu, D. A., Martins, J. V., et al. (2005). The MODIS aerosol algorithm, products and validation. *Journal of the Atmospheric Sciences*, *62*, 947−973.

Rothman, L. S., Jacquemart, D., Barbe, A., Benner, D. C., Brown, L. R., Carleer, M. R., et al. (2005). The HITRAN molecular spectroscopic database. *Journal of Quantitative Spectroscopy & Radiative Transfer*, *96*, 139−204.

Ruddick, K., De Cauwer, V., Park, Y., Becu, G., De Blauwe, J. -P., De Vreker, E., et al. (2003). Preliminary validation of MERIS water products for Belgian coastal waters. *Proceedings of Envisat Validation Workshop 2002* ESA SP-531.

Schneider, J., Ansmann, A., Baldasano, J., Balis, D., Bockmann, C., Bosenberg, J., et al. (2000). A European aerosol research lidar network to establish an aerosol climatology: EARLINET. *Journal of Aerosol Science*, *31*, 592−593.

Stamnes, K., Tsay, S. C., Wiscombe, W., & Jayaweera, K. (1988). Numerically stable algorithm for discrete-ordinate-method radiative transfer in multiple scattering and emitting layered media. *Applied Optics*, *27*, 2502−2509.

Vanbauce, C., Buriez, J. C., Parol, F., Bonnel, B., Sèze, G., & Couvert, P. (1998). Apparent pressure derived from ADEOS-POLDER observations in the oxygen A-band over ocean. *Geophysical Research Letters*, *25*, 3159−3162.

Van Diedenhoven, B., Hasekamp, O. P., & Aben, I. (2005). Surface pressure retrieval from SCIAMACHY measurements in the O_2 A-band: Validation of the measurements and sensitivity on aerosols. *Atmospheric Chemistry and. Physics Discussions*, *5*, 1469−1499.

Voss, K., Welton, E. J., Quinn, P. K., Johnson, J., Thompson, A., & Gordon, H. R. (2001). Lidar measurements during Aerosol99. *Journal of Geophysical Research*, *106*, 20,821−20,832.

Welton, E. J., & Campbell, J. R. (2002). Micropulse lidar signals: Uncertainties analysis. *Journal of Atmospheric and Oceanic Technology*, *19*, 2089−2094.

Winker, D. M., Hunt, W. H., & Hostetler, C. A. (2004). Status and performance of the CALIOP lidar. *Proceedings of SPIE*, *5575*, 8−15.

Winker, D. M., Pelon, J., & McCormick, M. P. (2003). The CALIPSO mission: Spaceborne lidar for observation of aerosols and clouds. In U. N. Singh, T. Itabe, & Z. Liu (Eds.), *Lidar remote sensing for industry and environment monitoring IIIProceedings of SPIE*, *Vol. 4893*. (pp. 1−11).

Zimmermann, G., Neumann, A., Sumnich, H., & Schwarzer, H. (1993). MOS/ PRIRODA—An imaging VIS/NIR spectrometer for ocean remote sensing. *Proceedings of SPIE*, *1937*, 201−206.

Zwally, H. J., Schutz, B., Abdalati, W., Abshire, J., Bentley, C., Brenner, A., et al. (2002). ICEsat's laser measurements of polar ice, atmosphere, ocean, and land. *Journal of Geodynamics*, *34*(3–4), 405−445.